University of Thi-Qar Journal of Science (UTsci)
ISSN Onlin:2709-0256, ISSN Print: 1991-8690 Volume (8), No.1

The utilisation of statistics to estimate evaporation from the surface of solar ponds

Asaad Hameed Sayer
Department of Chemistry/ College of Science/ University of Thi-Qar
Thi-Qar/ Iraq
assa.sayar@sci.utq.edu.iq
alimmz5@yahoo.com

Hazim Al-Hussaini
Department of Chemical and Process Engineering/ Faculty of Engineering and Physical Sciences/ University of Surrey GU2 7XH, UK
Guildford/ United Kingdoom
h.al-hussaini@surrey.ac.uk

Alasdair N. Campbell
Department of Chemical and Biological Engineering/ University of Sheffield S10 2TN
Sheffield/United Kingdoom
a.n.campbell@sheffield.ac.uk

Abstract*- Renewable energies including solar energy offer the best opportunity to decrease greenhouse gases and introduce the necessary solutions to meet demand for energy. Solar ponds are a simple, and cost-effective way to collect and store incident solar radiation. The most widely used type is the salinity gradient solar pond (SGSP), which can provide large capacity, and supply thermal heat for year-round for a wide range of applications. Evaporation has been shown previously to be the major mode of heat loss from the surface of the SGSP. In the present study, the utility of linear regression analysis to create a reasonable model to describe the evaporation level from the surface of an open water body is investigated. The created models considered the climatic factors (the ambient temperature, relative humidity, wind speed, and solar radiation). Evaporation levels were also calculated utilizing equation of Kishore and Joshi (1984). The calculated levels using the two created models and Kishore and Joshi's equation were compared with the measured evaporation at the local meteorological station for nine months. The results showed that good agreements were achieved, and the suggested statistical models could be used to calculate evaporation from the surface of a SGSP at any time when measurements of the ambient temperature, relative humidity, wind speed and solar radiation are available. The second model showed that solar radiation could be excluded from the calculation, and the results remained with an acceptable relative error.

Keywords—solar energy, evaporation, statistics, solar ponds

1. Introduction

With the serious challenge of climate change facing the world, it is essential to exploit renewable energies, helping reduce the impact of climate change by cutting emissions of greenhouse gases (GHG). Increasing investment in this energy sector worldwide could significantly enhance the environment. Keles and Bilgen (2012) implied that renewables offer the best opportunity to reduce greenhouse gases and introduce sustainable and desirable solutions to the increasing demand for energy. Human health is threatened by the high levels of pollution resulting from the utilisation of conventional fossil fuels for energy generation; limiting the use of these energy sources is therefore a significant aim. Economic development has been positively correlated with the increase in both energy use and GHG emissions. Renewable energy can undoubtedly change that correlation since renewables are sustainable with low or no GHG emissions (Edenhofer et al., 2012; and Sayer and Mahood, 2020). parentheses, following the example. Some components, such as multi-leveled equations, graphics, and tables are not prescribed, although the various table text styles are provided. The formatter will need to create these components, incorporating the applicable criteria that follow.

A. Salinity gradient solar pond

The benefits of any energy source must be assessed not only in terms of economics but also in terms of its short-and long-term impacts on ecology and human life. Solar power-based technologies could be the most natural form of energy harvesting, offering unlimited power generation for as long as the sun shines on the surface of our planet (Gevorkian, 2012; Gevorkian, 2016; and Napoleon and Akbarzadeh, 2013). Most technologies linked to power generation, including electrical power generated from conventional fuels, atomic energy or biofuel, require a constant supply of feedstock. On the other hand, solar energy uses natural resources to generate electricity, with no need for fuel or feedstock. The technologies convert the abundant energy of the sun into useful power.

Among the different applications of solar energy is the solar ponds. There are several types of solar ponds. The most significant type is the salinity gradient solar pond (SGSP) (Sayer et al., 2016). Salinity gradient solar ponds are globally constructed and implemented for many different purposes. They can supply thermal energy to a wide range of applications that require low-grade heat to run (Karakilcik et al., 2006; Ziapour et al., 2016; Ruskowitz et al., 2014; Alrowaished et al., 2013; Caruso and Naviglio, 1999; Dehghan et al., 2013; Kurt et al., 2000; Assari et al., 2017; Abbassi Monjezi, and Campbell, 2016; Abbassi Monjezi et al., 2017; Amigo et al., 2017; Torkmahalleh et al., 2017; and Khalilian, 2017).

A salinity gradient solar pond can be defined as a body of water with a depth of 2-5 m and a gradient of salt concentration. It consists of three distinct zones: the surface layer or the upper convective zone (UCZ), the middle layer or the non-convective zone (NCZ) and the lower convective zone (LCZ). The UCZ is approximately homogenous, and it is a relatively cold layer made from freshwater or low salinity brine. The NCZ has a salinity gradient i.e. the salinity increases from the top to the bottom of the layer (Sayer et al., 2016; Sayer et al., 2018; Jaefarzadeh, 2004; and Jahromy, 2016). The SGSP is a simple means of collecting and storing solar energy; it receives and stores solar radiation in its lower layer due to the suppression of convection (Hull et al., 1984; Nielsen, 1975; and Babaei et al., 2021). To prevent convection, salty solution (water) is used in the solar ponds. Therefore, these ponds are named salinity gradient solar pond (Velmurugan and Srithar, 2008; Tundee et al., 2010; Weinberg and Doron, 2010; and Kumar and Das, 2021). A schematic of the SGSP is illustrated in Figure 1, it shows that convection occurs in the UCZ and the LCZ while it is suppressed in the NCZ due to the salinity (density) gradient.

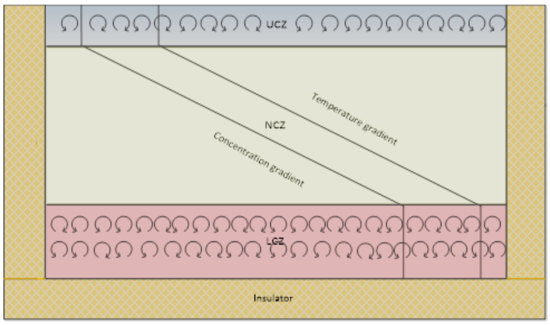

Figure 1: Schematic diagram of a salinity gradient solar pond (SGSP). The pond is surrounded by an insulator to minimize the heat loss, particularly from the bottom, the pond zones are the UCZ, the NCZ, and the bottom layer (LCZ), convection currents only in the top and bottom layers.

The NCZ is a transparent insulating layer, and its existence is the key to the operation of a SGSP (Lu et al., 2004; Karakilcik et al., 2013; Valderrama et al., 2011; Sayer et al., 2017b; Suarez et al., 2014; sayer et al., 2019; and Sathish and Jegadheeswaran, 2021).

B. *Evaporation*

Evaporation is one of the main challenges in reservoirs around the world, in particular, in areas have hot and arid weathers. Therefore, reducing the level of evaporation has become an essential target, particularly in areas of little rainfall and low runoff, and simultaneously have plentiful of solar radiation (Assouline et al., 2010; Silva et al., 2017; Bozkurt et al., 2012; and Sayer et al., 2017). Covering the open water body with opaque floating materials is an effective way to diminish evaporation from the surface. However, these materials will not allow solar radiation to penetrate into the water body, and thus, they are not beneficial to do such work for solar ponds.

In solar ponds, many studies were achieved to eliminate or decrease evaporation from these ponds (Silva et al., 2017; Assari et al., 2015; Ruskowitz et al., 2014; and Sayer et al., 2017). It was concluded that reducing evaporation has increased the performance of the pond (the temperature of the LCZ). Moreover, Ruskowitz et al. (2014) observed that when evaporation was decreased, there was an increase in the UCZ temperature. Sayer et al. (2016) found that surface heat loss from a SGSP by evaporation was significant while the radiation heat loss was small. Their theoretical results showed that suppressing surface evaporation would substantially increase temperatures in the UCZ and LCZ.

This paper does not endeavour the suppression of evaporation, but it highlights the utilisation of the linear regression analysis to find a straightforward and accurate formula to estimate evaporation from the surface of an open water body. The measurements of 9 months and the statistical analysis presented in Sayer et al. (2017) have been used. Their findings were extended to find a suitable model which describes the evaporation from open water bodies including solar ponds.

II. Results and discussion

A. *Regression analysis*

To find a relationship which can gather all climatic factors together with the evaporation, a statistical analysis was performed by Sayer et al. (2017) on an extended period measurements (9 months) to find this relationship. Their statistical data which were generated using a multiple linear regression analysis is given in Table 1.

Table 1: Statistical data of multiple regression analysis (Sayer et al., 2017)

R^2= 0.81156, $AdjR^2$ = 0.80838

	Coefficients	*Standard Error*	*t Stat*	*P-value*
Intercept	-1.2234	1.882396	-0.64992	0.516375
Solar radiation (*H*)	0.106939	0.059791	1.788545	0.074965
Ambient temperature (T_a)	0.380862	0.045975	8.284036	8.81E-15
Relative humidity (γ_h)	-9.31657	2.287592	-4.07265	6.34E-05
Wind Speed (v)	0.412576	0.123479	3.341269	0.000969

Table 1 shows that evaporation can be predicted by the following equation:

$$Ev = -1.2234 + 0.106939H + 0.380862T_a - 9.31657\gamma_h + 0.412576\mathrm{v} \tag{1}$$

The evaporation calculated by Model 1 (Equation 1) is plotted against the measured evaporation presented in Sayer et al. (2017), and the results are illustrated in Figure 2(a). For more investigation to the suitability of Model 1, the predicted evaporation by the model is plotted against the residuals (residual= measured value – predicted value). The results are shown in Figure 2(b).

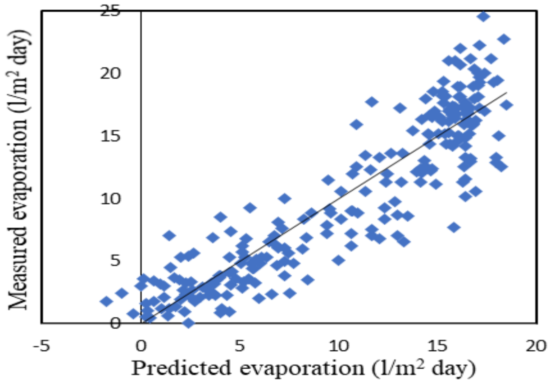

(a)

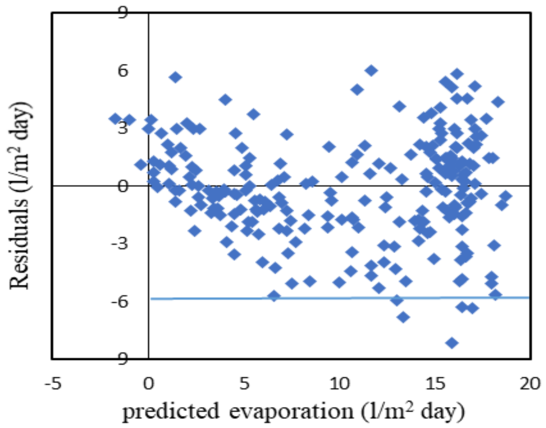

(b)

Figure 2: The results when all parameters affecting evaporation are considered, (a) the predicted results against the measured values, (b) the predicted evaporation against the residuals.

Figure 2(a) illustrates that Model 1 (Equation 1) gives an acceptable estimation to the evaporation level, points scatter in an approximately narrow area around the fitted line. Figure 2(b) also shows that points dispersed randomly around the zero horizontal line of the residuals, and the variation is between -6 and 6.

It is also beneficial to plot separately the independent variables with the residuals to observe the distribution of points around the zero line. Consequently, the four factors are plotted against the residuals and the results are illustrated in Figure 3.

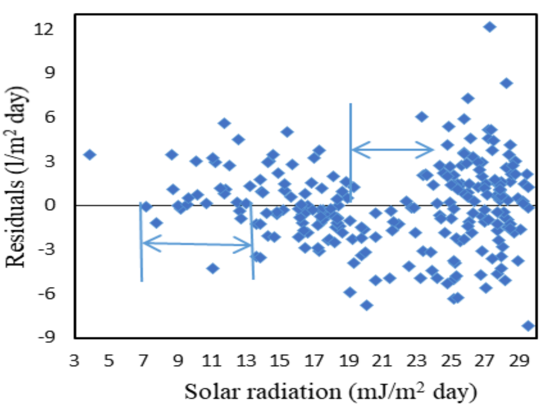

(a)

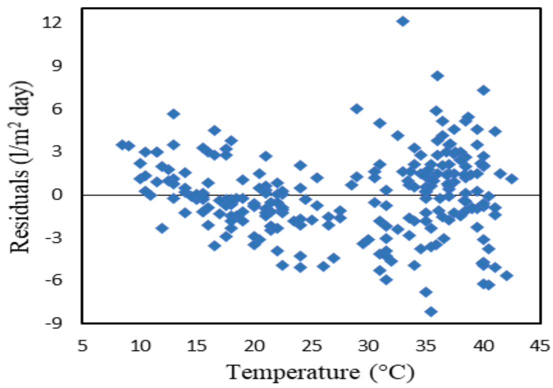

(b)

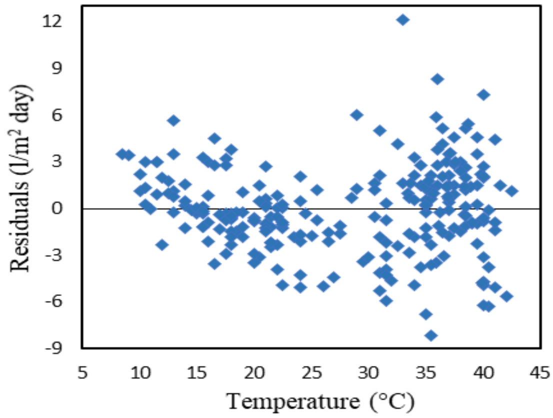

(c)

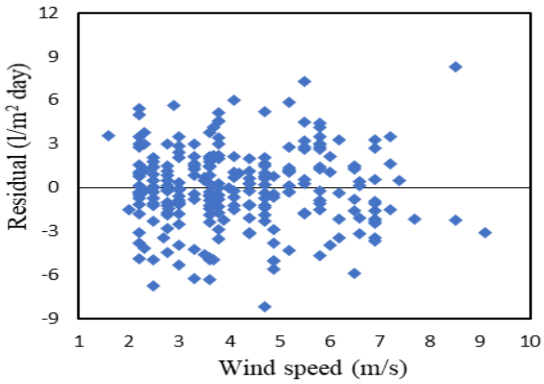

(d)

Figure 3: The residuals against the four meteorological parameters, (a) the solar radiation with the residuals, (b) the ambient temperature with the residuals, (c) the relative humidity against the residuals, and (d) the wind speed against the residuals.

It is known in statistics that when points are randomly dispersed around the horizontal axis, a linear regression model is appropriate, otherwise, the model is unacceptable (Petruccelli et al., 1999, Freedman et al., 1998). Figure 3 shows that the points' distribution around zero horizontal line is reasonable except the case with the solar radiation (Figure 3(a)). In the case of the solar radiation, the scattering is not uniform around the zero line. For example, from 7 -13 mJ/m2 day (on the horizontal axis), it can be seen that points concentrated above the horizontal line and the area below the line is empty. Moreover, from 19-23 mJ/m2 day on the same axis, points condensed below the line, and there are approximately no points above the line (Figure 3(a)).

Moreover, Table 1 shows that all of the climatic factors have a statistically significant impact on the model ($p < 0.001$) except for the solar radiation, which is not significant even at $p < 0.05$.

The value of R2 represents the deviation of measured evaporation from the predicted evaporation by the model. When a new variable is added to the regression analysis, the value of R^2 might increase. On the other hand, this increase in R2 does not mean that the accuracy of the model increases. As known that the adjusted R^2 (AdjR^2) is more accurate than R^2, and it is calculated as follows:

$$AdjR^2 = 1 - (1 - R^2)\frac{n-1}{n-k-1} \tag{2}$$

where n is the number of observations, and k is the number of variables. If a useful variable is added to the statistical analysis, the value of $AdjR^2$ will increase. However, if the added variable is insignificant, there will be no enhancement in the $AdjR^2$.

In their regression analysis (Sayer et al., 2017), the solar radiation was excluded and the analysis performed again. The results are given in Table 2.

Table 2: Statistical data of multiple regression analysis (incident solar radiation is excluded, Sayer et al., 2017)

R^2= 0.809017, $AdjR^2$= 0. 0.80661

	Coefficients	*Standard Error*	*t Stat*	*P-value*
Intercept	-0.146	1.791627	-0.08149	0.935118
Ambient temperature (T_a)	0.42634	0.03848	11.07939	2.81E-23
Relative humidity (γ_h)	-10.0035	2.265518	-4.41553	1.53E-05
Wind Speed (v)	0.45441	0.121802	3.730722	0.000239

A new model can be written depending on the results of Table 2, and it is as follows:

$$Ev = -0.146 + 0.42634T_a - 10.0035\gamma_h + 0.454416v \tag{3}$$

The predicted evaporation by Equation 3 (Model 2) is plotted against the measured evaporation; the results are illustrated in Figure 4(a). Similar to the previous model (when all parameters are considered), the results gathered using Model 2 (Equation 3) are plotted against the residuals and shown in Figure 4(b).

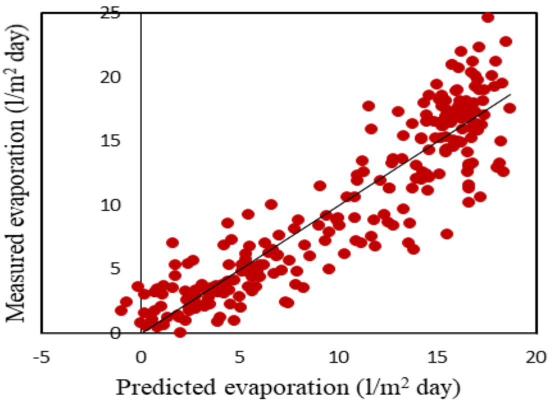

(a)

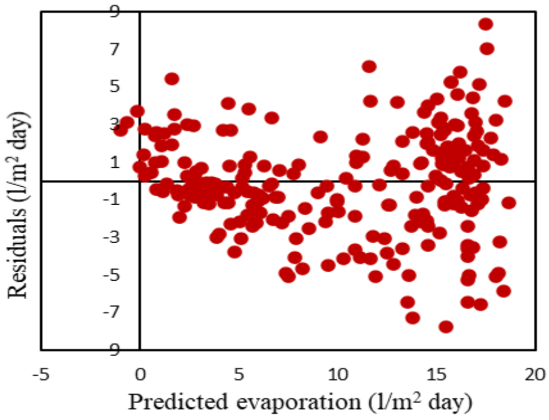

(b)

Figure 4: The results when the solar radiation is excluded, (a) the predicted results against the measured values, (b) the predicted evaporation against the residuals.

Figure 4 (a and b) shows that this model could introduce satisfactory results even with the exclusion of the solar radiation. Figure 4(b) also shows that points distributed randomly up and down the zero horizontal line, and the variation is mostly between -5 and 5.

Similar to the case when the four parameters were considered; the three measured parameters are plotted against the residuals. The results are illustrated in Figure 5 (a), (b), and (c).

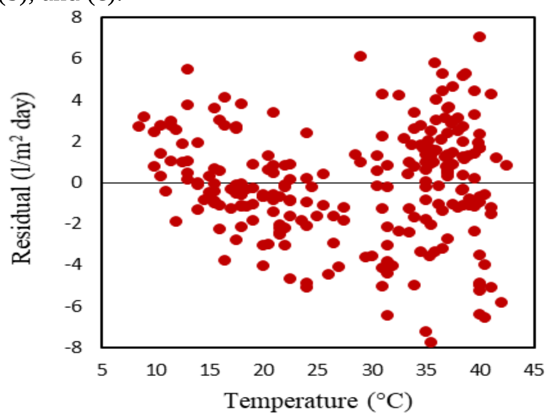

(a)

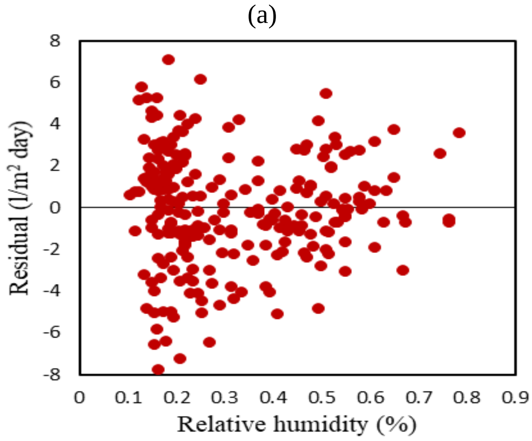

(b)

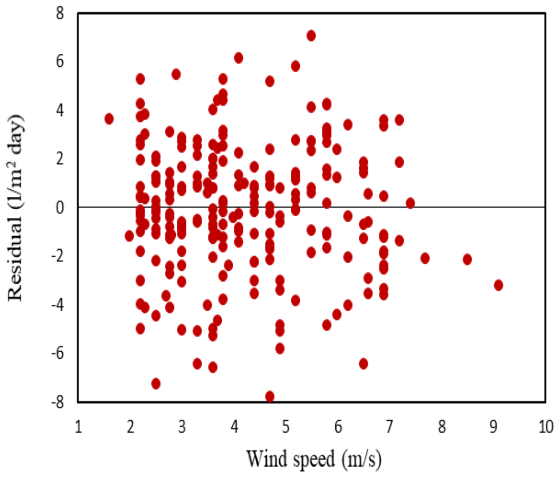

(c)

Figure 5: Points distribution of the three meteorological parameters (the solar radiation is excluded) around the horizontal line, (a) the ambient temperature with the residuals, (b) the relative humidity against the residuals, and (c) the wind speed against the residuals.

It is evident from Figure 5(a), (b), and (c) that for the three considered parameters, points are scattered on both sides of the zero horizontal line. This means that the model can be used to predict the evaporation in the area of the study at any time. Interestingly, Table 2 shows that there is a slight reduction in the value of both R^2 and $AdjR^2$. This means that solar radiation can be excluded from the fitted model.

B. *The comparison of calculated evaporation levels with the measurements*

Kishore and Joshi (1984) suggested an equation to calculate the evaporation from the surface of the water body. It is commonly used in the calculation of evaporation from the surface of the SGSP; it is as follows:

$$Q_{ue} = \left\{\frac{[\lambda h_c(p_u - p_a)]}{[(1.6 C_s p_{atm})]}\right\} \quad (4)$$

where C_s is the humid heat capacity of air in kJ/kg. K, given by:

$$C_s = 1.005 + 1.82\gamma_h \quad (5)$$

The symbol λ represents the latent heat of vaporisation in kJ/kg, p_u is the water vapour pressure at the upper layer temperature in mmHg and it is calculated as:

$$p_u = exp[18.403 - 3885/(T_u + 230)] \quad (6)$$

The partial pressure of water vapour in the ambient temperature in mmHg is represented by p_a and it is calculated as:

$$p_a = \gamma_h exp[18.403 - 3885/(T_a + 230)] \quad (7)$$

The symbol p_{atm} is the atmospheric pressure in mmHg, and γ_h is the relative humidity.

The evaporation levels for the considered 9 months (January- September) were calculated using Kishore and Joshi's equation (1984), and the results are compared with the available evaporation measurements for those months. Evaporation was also calculated using Models 1 and 2 and compared with the measurements. The comparisons are illustrated in Figure 6.

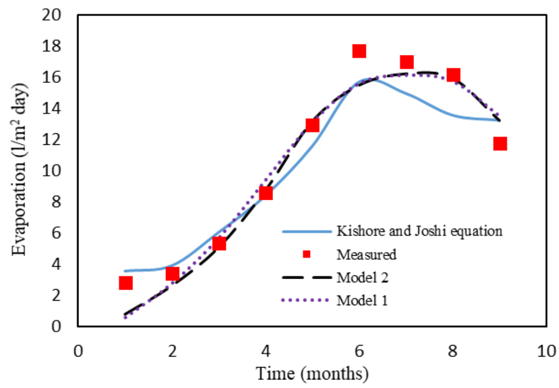

Figure 6: The comparison between the experimental measurements and the theoretical evaporation (calculated by the Kishore and Joshi's equation, Model 1, and Model 2) levels (month 1 is January).

Figure 6 shows that the theoretical trend is approximately similar to the measured trend for the considered nine months. The relative errors between the measured and the calculated results, which are represented in Figure 6, are given in Table 3.

Table 3: The relative errors between the theoretical calculations and the experimental measurements of the evaporation for 9 months (January-September); the theoretical values were calculated using Kishore and Joshi's equation, Model 1, and Model 2.

Month	1	2	3	4	5	6	7	8	9	Average
Relative error										
Kishore and Joshi's equation	0.20	0.14	0.13	0.01	0.10	0.11	0.11	0.16	0.12	0.10
Statistical equation (Model 1)	0.7	0.18	0.06	0.1	0.01	0.1	0.05	0.02	0.14	0.15
Statistical equation (Model 2)	0.7	0.2	0.04	0.02	0.01	0.1	0.04	0.01	0.12	0.13

Table 3 illustrates that the average relative errors are 0.1, 0.15, and 0.13 for Kishore and Joshi's equation, Model 1, and Model 2 respectively. These values are reasonable. Figure 6 and Table 3 also show that models 1 and 2 could be used to calculate evaporation from the surface of the pond. Model 2 requires only knowledge of the ambient temperature, relative humidity, and wind speed. The daily rate of evaporation per month for the whole year in the area of the study is calculated using the three equations. The results are shown in Figure 7.

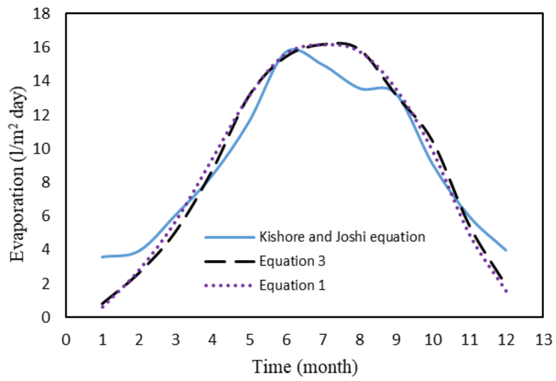

Figure 7: The theoretical evaporation rates during one year calculated by Kishore and Joshi's equation (1984), Model 1 (Equation 1), and Model 2 (Equation 3) in the site of the experiment (Nasiriyah City) (month 1 is January).

Figure 7 shows that in the area of the study, the evaporation level is relatively low during months of January, February, March, November, and December. Evaporation levels throughout these months are below 6 l/m2 day. For the rest months of the year (7 months), it is apparent that evaporation levels are approximately high.

III. Conclusion

This paper has been investigated the use of the regression analysis to generate a suitable model to describe the evaporation level from the surface of an open water body. Measurements of 9 months presented in Sayer et al. (2017) have been considered to find the model. The linear regression analysis has been used to generate two models to calculate the evaporation from the surface of the open water bodies including solar ponds. These models depended only on the climatic factors (the ambient temperature, relative humidity, wind speed, and solar radiation). Evaporation levels were also calculated utilizing Kishore and Joshi equation (1984). The calculated levels were compared with the measured levels for the considered nine months and acceptable agreements were achieved for the two statistical models and also for the Kishore and Joshi's equation. Moreover, the results illustrated that the statistical model when the solar radiation was excluded gave a reasonable agreement with a relative error of 13%.

References

Abbassi Monjezi A., Campbell A. N., 2016. A comprehensive transient model for the prediction of the temperature distribution in a solar pond under Mediterranean conditions. Solar Energy 135, 297–307.

Abbassi Monjezi, A., Mahood, H.B., Campbell, A.N., 2017b. Regeneration of dimethyl ether as a draw solute in forward osmosis by utilising thermal energy from a solar pond. Desalination 415, 104–114

Alrowaished, A., Azni, I., Mohamed, T. A., Amimul, A., 2013. The development and applications of solar pond: a review. Desalination & Water Treatment 10, 1–13.

Amigo, J., Meza, F., Suárez, F., 2017. A transient model for temperature prediction in a salt-gradient solar pond and the ground beneath it. Energy, DOI: 10.1016/j.energy.2017.05.063

Assari, M. R., Tabrizi, H. B., Nejad, A. K., Parvar, M., 2015. Experimental investigation of heat absorption of different solar pond shapes covered with glazing plastic. Sol. Energy 122, 569–578.

Assari, M. R., Tabrizi, H. B., Parvar, M., Nejad, A. K., Jafar Gholi Beik, A., 2017. Experiment and optimization of mixed medium effect on small-scale salt gradient solar pond. Solar Energy, 151, 102-109.

Assouline, S., Narkis, K., Or, D., 2010. Evaporation from partially covered water surfaces. Water Resources Research 46, W10539. http:// dx.doi.org/10.1029/2010WR009121.

Babaei, H.R., Khoshvaght-Aliabadi, M., Mazloumi, S.H., 2021. Analysis of serpentine coil with alternating flattened axis: An insight into performance enhancement of solar ponds. Solar Energy, 217, pp.292-307.

Bozkurt, I., Karakilcik, M., 2012. The daily performance of a solar pond integrated with solar collectors. Solar Energy 86, 1611-1620.

Caruso, A., Navigilio, A., 1999. Desalination plant using solar heat as a heat supply, not affecting the environment with chemicals. Desalination 122, 225–234.

Dehghan, A. A., Movahedi, A., Mazidi, M., 2013. Experimental investigation of energy and energy performance of square and circular solar ponds. Solar energy 97, 273-284.

Freedman, D., Pisani, R., Purves, R., 1998. Statistics, third edition, printed in the United State of America, Norton & company, Inc.

Gevorkian, P., 2012. Large scale solar power systems, construction and economics. Cambridge University press. New York, USA.

Gevorkian, P., 2016. Solar power generation problems, solutions, and monitoring. Cambridge University, ISBN 978-1-107-12037-2

Hull, J.R., Liu, K.V., Sha, W.T., Jyoti, K., Nielsen, C.E., 1984. Dependence of ground heat loss upon solar pond size and perimeter insulation, calculated and experimental results. Sol. Energy 33 (1), 25-33.

Edenhofer, O.,PichsMadruga, R.,Sokona,Y., Seyboth, K., Matschoss, P., Kadner, S., Zwickel, T., Eickemeier, P., Hansen,G., Schl¨omer, S., Stechow, C., 2011. IPCC Special Report on Renewable Energy Sources and Climate Change Mitigation. Reprinted with corrections in 2012.

Jaefarzadeh, M.R., 2004. Thermal behaviour of a small salinity-gradient solar pond with wall shading effect. Sol. Energy 77, 281-290.

Jahromy, R., 2016. Study of net heat absorbed or lost in non-convective zone of a solar pond. International Academic Journal of Science and Engineering 3 (5), 1–10. ISSN 2454-3896

Karakilcik, M., Dincer, I., Marc, A.R., 2006. Performance investigation of a solar pond. Appl. Therm. Eng. 26, 727-735.

Karakilcik, M., Dincer, I., Bozkurt, I., Atiz, A., 2013. Performance assessment of a solar pond with and without shading effect. Energy Conversion and Management 65, 98-107.

Keles, S., Bilgen, S., 2012. Renewable energy sources in Turkey for climate change mitigation and energy sustainability. Renewable and Sustainable Energy Reviews, 16, 5199-5206.

Khalilian, M., 2017. Experimental investigation and theoretical modeling of heat transfer in circular solar ponds by lumped capacitance model. Applied Thermal Engineering/ DOI: http://dx.doi.org/10.1016/j.applthermaleng.2017.04.129

Kishore, V.V.N., Joshi, V., 1984. A practical collector efficiency equation for non-convecting solar ponds. Sol. Energy 33 (5), 391-395.

Kumar, A., Das, R., 2021. Effect of peripheral heat conduction in salt-gradient solar ponds. Journal of Energy Storage, 33, p.102084.

Kurt, H., Halici, F., Binark, A. K., 2000. Solar pond conception - experimental and theoretical studies. Energy Conversion & Management 41, 939-951.

Lu, H., John, C.W., Andrew, H.P., Herbert, D.H., 2004. Advancements in salinity gradient solar pond technology based on sixteen years of operational experience. J. Sol. Energy Eng. 126, 759-767.

Napoleon, E., Akbarzadeh, A., 2013. Physics of solar energy and its applications. In: Napoleon, E., Akbarzadeh, A. (Eds.), Solar Energy Sciences and Engineering Applications. CRC press. E. Book.

Nielsen, E.C., 1975. Salt-Gradient Solar Ponds for Solar Energy Utilization, Environmental Conservation. The Foundation of Environmental Conservation, Vol. 2, No. 4, printed in Switzerland.

Petruccelli, J. D., Nandram, B., Chen, M., 1999. Applied statistics for engineers and scientists. Prentice-Hall, Inc, printed in the United State of America.

Ruskowitz, J. A., Suarez, F., Tyler, S. W., Childress, A. E., 2014. Evaporation suppression and solar energy collection in a salt-gradient solar pond. Sol. Energy 99, 36–46.

Sathish, D., Jegadheeswaran, S., 2021. Evolution and novel accomplishments of solar pond, desalination and pond coupled to desalination systems: a review. J Therm Anal Calorim. https://doi.org/10.1007/s10973-021-10579-8

Sayer, A. H., Al- Hussaini H., Campbell, A. N., 2016. New theoretical modelling of heat transfer in solar ponds. Sol. Energy 125, 207–218.

Sayer, A. H., Al-Hussaini, H., Campbell, A. N., 2017. Experimental analysis of the temperature and concentration profiles in a salinity gradient solar pond with, and without a liquid cover to suppress evaporation, Solar Energy 155, 1354-1365.

Sayer, A. H., Al-Hussaini, H., Campbell, A. N., 2017b. An analytical estimation of salt concentration in the upper and lower convective zones of a salinity gradient solar pond with either a pond with vertical walls or trapezoidal cross section, Solar Energy 158, 207-2017.

Sayer, A. H., Al-Hussaini, H., Campbell, A. N., 2018. New comprehensive investigation on the feasibility of the gel solar pond, and a comparison with the salinity gradient solar pond, Applied Thermal Engineering 130, 672-683.

Sayer, A. H., Monjezi, A. A., Al-Hussaini, H., Campbell, A. N., 2019. Experimental and theoretical investigation of the temperature and concentration distributions of the upper and lower convective zones of a small salinity gradient solar pond covered with a thin liquid layer. Conference paper, IAPE '19, Oxford, United Kingdom ISBN: 978-1-912532-05-6.

Sayer, A. H., Mahood, H. B, 2020. Improved Thermal Efficiency of Salinity Gradient Solar Pond by Suppressing Surface Evaporation Using an Air Layer. Energy Engineering 117(6), 367–379.

Silva, C., Gonzalez, D., Suarez, F., 2017. An experimental and numerical study of evaporation reduction in a salt-gradient solar pond using floating discs. Sol. energy 142, 204–214.

Suarez, F., Ruskowitz, J. A., Childress, A. E., Tyler, S. W., 2014. Understanding the expected performance of large –scale solar ponds from laboratory–scale observations and numerical modelling. Applied Energy 117, 1-10.

Torkmahalleh, M. A., Askari, M., Gorjinezhad, S., Eroglu, D., Obaidullah, M., Habib, A. R., Godelek, S., Kadyrov, S., Kahraman, O., Pakzad, N. Z., Ahmadi, G., 2017. Key factors impacting performance of a salinity gradient solar pond exposed to Mediterranean climate. Sol. Energy 142, 321–329

Tundee, S., Terdtoon, P., Phrut, S., Singh, R., Akbarzadeh, A., 2010. Heat extraction from salinity-gradient solar ponds using heat pipe heat exchangers. Solar Energy 84, 1706-1716.
Valderrama, C., Gibert, O., Arcal, J., Solano, P., Akbarzadeh, A., Larrotcha, E., Cortina, J., 2011. Solar energy storage by salinity gradient solar pond: Pilot plant construction and gradient control. Desalination 279, 445-450.
Velmurugan, V., Srithar, K., 2008. Prospects and scopes of solar pond: a detailed review. Renew. Sustain. Energy Rev. 12, 2253-2263.
Weinberg, J., Doron, B., 2010. Desalination and Water Resources, Renewable Energy System and Desalination. E-Book, ISBN: 978-1-84826-430-4.
Ziapour, B. M., Shokrnia, M., Naseri, M., 2016. Comparatively study between single-phase and two-phase modes of energy extraction in a salinity-gradient solar pond power plant. Energy 111, 126–136.